

Single quantum dot photocurrent spectroscopy in the cavity quantum electrodynamics regime

P. Gold, M. Gschrey,* C. Schneider, S. Höfling, A. Forchel, M. Kamp, and S. Reitzenstein*[†]

Technische Physik and Wilhelm Conrad Röntgen Research Center for Complex Material Systems, Physikalisches Institut, Universität Würzburg, Am Hubland, D-97074 Würzburg, Germany

(Received 5 June 2012; published 1 October 2012)

We study cavity quantum electrodynamics (cQED) in coupled quantum dot–microcavity systems under electrical readout. Strict resonant excitation of a target quantum dot (QD) allows us to monitor the photocurrent response of a single emitter in the quantum limit of light–matter interaction. We find a strong anticorrelation between radiative recombination and nonradiative tunnel escape of photoexcited carries which can be controlled by cQED effects in the Purcell regime. In fact, cavity-enhanced radiative emission from a QD results in a weaker photocurrent signal which reflects the cQED controlled competition between radiative and nonradiative recombination at the single emitter level.

DOI: [10.1103/PhysRevB.86.161301](https://doi.org/10.1103/PhysRevB.86.161301)

PACS number(s): 78.67.Hc, 42.50.Ct, 42.50.Pq, 85.60.–q

The interaction of light and matter at the quantum level is one of the most fundamental and attractive topics of modern semiconductor nanoscience. Both the incoherent weak coupling regime and the coherent strong coupling regime in the framework of cavity quantum electrodynamics (cQED) are very appealing for fundamental research and applications in quantum science and technology.^{1–3} For instance, the weak coupling effect has been exploited to enhance the extraction efficiency of quantum dot (QD) based single photon sources.^{4–6} Moreover, intriguing phenomena such as the nonresonant coupling effect between spectrally detuned QD emission lines and the optical mode of high quality factor (Q) microcavities^{7,8} have been identified in recent years. Most of these studies have been performed either by standard microphotoluminescence (μ PL) or microelectroluminescence (μ EL) spectroscopy. More recently, also coherent excitation in reflection geometry^{9,10} or resonance fluorescence^{11,12} have been applied to study coupled QD–microcavity systems.

Single QD photocurrent (PC) spectroscopy presents a complementary and very attractive method to explore single emitter cQED effects and to electrically read out information from a coupled QD–microcavity system. The high potential of the photocurrent technique for the investigation and control of quantum systems has already been demonstrated in a number of important works based on simple QD–Schottky diodes.^{13–17} This includes, for instance, the coherent manipulation and readout of a QD acting as a two-level system and the observation of Ramsey fringes.¹⁸

We report insights into light–matter interaction on the single emitter level by applying single QD PC spectroscopy in the cQED regime. In order to address single QDs, we excite a coupled QD–microcavity system under strict resonant conditions, which allows us to select specific QDs and to read out their occupation electrically. Temperature tuning experiments allow us to control the radiative lifetime τ_r of a selected QD exciton in the weak coupling regime with strong implications on the associated PC. Indeed, the competition between tunnel escape and radiative recombination at the single QD level leads to a reduction of photocurrent when enhanced radiative recombination occurs on resonance with the cavity mode (see Fig. 1).

In order to study single QD PC effects in the cQED regime, we fabricated electrically contacted, high- Q QD micropillar

cavities based on AlAs/GaAs microcavity samples with a single layer of $\text{In}_x\text{Ga}_{1-x}\text{As}$ QDs in the active region. Electron beam lithography and reactive ion plasma etching were used to pattern and contact micropillars with diameters between 1.5 and 2.0 μm . Details on the fabrication process are given in Ref. 19. The micropillars were investigated at low temperature between 10 and 50 K inside a He-flow cryostat. A tunable semiconductor laser with a linewidth of 100 kHz was used to excite single micropillars either from the top in the normal orientation to the sample’s surface or via sidewall excitation at an angle of 70° with respect to the normal direction. For laser beam focusing and detection of luminescence in normal direction a microscope objective with a numerical aperture (NA) of 0.4 was used. The photocurrent was detected by the lock-in technique under an applied dc bias voltage. In addition, a high resolution spectrometer (spectral resolution 16 μeV) was used to detect PL from the structures under nonresonant excitation at 842 nm.

At first, let us focus on PC features of a coupled QD–micropillar system under side excitation. In this case, one can neglect the spectral selectivity of the microresonator which modulates the effective excitation power under top excitation (see below). Figure 2(a) shows a representative single QD PC spectrum obtained from a micropillar with a diameter of 2.0 μm at an excitation power of 30 μW and a bias voltage of $V_{\text{bias}} = -1$ V ($T = 40$ K). The spectrum was obtained by scanning the wavelength of the tunable diode laser and measuring the corresponding PC. In the PC spectrum we observe three distinct peaks which are associated with two single QD excitons (X1 and X2) and the fundamental optical mode (C) of the micropillar cavity. The excitonic signals have an asymmetric line shape with a low energy tail which could indicate a coupling to extended wetting layer states via a Fano-like resonance.²⁰ Interestingly, it is not expected to detect signatures of a photonic mode in a PC spectrum in the first place. In the present case, the cavity-related signal C is attributed to the prominent nonresonant QD–cavity coupling mechanism which has initially been identified in PL experiments^{7,8} and more recently also been applied as a monitor for single QD spectroscopy in resonance fluorescence.²¹ As a result of this mechanism, spectrally detuned QDs contribute to PC when the exciting laser is on resonance with the cavity mode which in turn explains the cavity related signal C in Fig. 2(a).

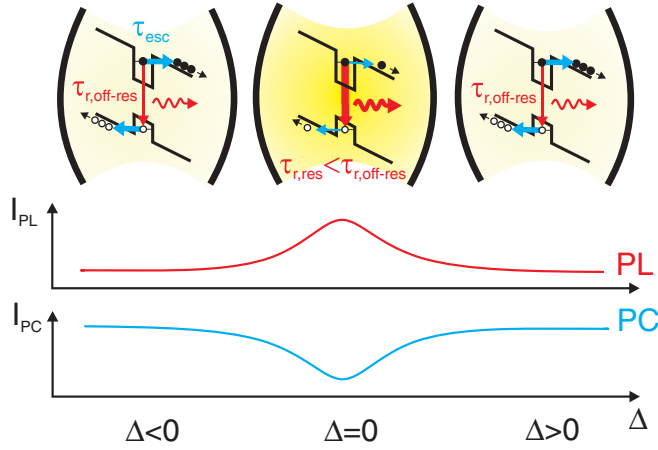


FIG. 1. (Color online) Schematic band diagram, PL intensity and resulting PC of a QD inside the active layer of a micropillar cavity under reverse bias for different detunings between the resonator mode and the QD exciton. The photoexcited charge carriers leave the QD by either tunnel emission or radiative recombination, depending on the tunnel (τ_{esc}) and recombination lifetime ($\tau_r(\Delta)$). In the weak coupling regime, $\tau_r(\Delta)$ is reduced on resonance ($\Delta = 0$) due to the Purcell effect. This leads to an increase in PL intensity (red line) and a corresponding reduction of PC (blue line).

The photocurrent response of a single QD under resonant optical excitation and different bias voltages can be described within a rate-equation approach which considers the QD as a simple two-level system.¹³ Within this approach the PC is given by

$$I = e \frac{N_0}{\tau_{\text{esc}}} = \frac{e}{2\tau_{\text{esc}}} \frac{\alpha P}{\alpha P + \left(\frac{1}{\tau_{\text{esc}}} + \frac{1}{\tau_r(\Delta)}\right)}, \quad (1)$$

where e denotes the electron charge, N_0 the steady state occupation of the QD by an exciton, τ_{esc} the tunneling time, P the excitation power, and α a proportional factor, to take into account stimulated emission processes.¹³ Equation (1) implies a saturation current of $I_{\text{sat}} = e/(2\tau_{\text{esc}})$. To account for cavity effects we introduced a radiative lifetime of the emitter τ_r which depends on the spectral detuning Δ of the emitter and

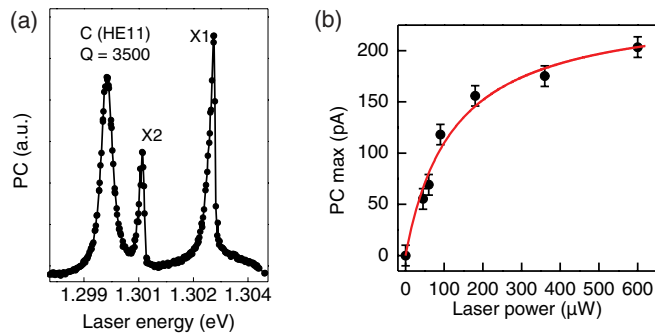


FIG. 2. (Color online) (a) High resolution PC spectrum of a QD micropillar with a diameter of $d_c = 2.0 \mu\text{m}$. The PC signals are associated with single QDs (X1 and X2) and with the fundamental cavity mode (C) of the micropillar. (b) Maximum of the PC signal from a single, off-resonant QD as a function of excitation power for a bias voltage of $V_{\text{bias}} = 0 \text{ V}$. Modeling (solid line) of the experimental data (bullets) yields a tunnel time of $\tau_{\text{esc}} = 330 \text{ ps}$.

the cavity mode via the Purcell effect as we will detail below. This model can be applied in order to describe the PC response of QDs in the present cavity system as can be seen in Fig. 2(b). Here the maximum PC of an off-resonant QD exciton line is plotted as a function of the laser power. Saturation of the single QD PC signal is clearly visible and the power dependence can be quantitatively reproduced by data calculated according to Eq. (1) [solid line in Fig. 2(b)] and yields a tunneling time of $\tau_{\text{esc}} = 330 \text{ ps}$ for a bias voltage of $V_{\text{bias}} = 0 \text{ V}$.

In the presence of a microcavity the PC signal depends on the detuning between a single QD and the confined optical mode, and it is necessary to extend Eq. (1) by introducing cQED effects. In the weak coupling regime it is essential to take into account that τ_r depends Δ via

$$\tau_r(\Delta) = \frac{\tau_{\text{bulk}}}{F_P \frac{\gamma_C^2}{4\Delta^2 + \gamma_C^2}}. \quad (2)$$

Here, the Purcell factor F_P is proportional to the quotient of the Q factor and the mode volume of the relevant cavity mode,²² τ_{bulk} refers to the spontaneous emission lifetime of the QD in bulk material, and γ_C denotes the linewidth (FWHM) of the cavity mode. According to Eq. (2), τ_r is reduced in resonance ($\Delta = 0$), which leads to enhanced radiative recombination. Thus, below saturation it is clear that the PC depends on the detuning via cQED effects and is expected to decrease for ($|\Delta| \rightarrow 0$) due to the competition between radiative recombination and tunnel escape of charge carriers from the QD.

Single QD cQED effects in PC are studied for a QD-micropillar system ($Q = 7000$, $d_c = 1.8 \mu\text{m}$, $\text{In}_{0.3}\text{Ga}_{0.7}\text{As}$ QDs as the active layer) under side excitation. The corresponding temperature dependent PC intensity map is presented in Fig. 3(a) for $P = 180 \mu\text{W}$ and $V_{\text{bias}} = 0 \text{ V}$. With increasing temperature from 32 to 42 K the QD line X shifts through resonance with the fundamental cavity mode C. It is nicely seen that the PC signal decreases when X crosses C at about 38 K. This is exactly what is expected according to Eqs. (1) and (2) which predict a decrease of the PC at resonance when radiative recombination is accelerated due to the Purcell effect.

For a quantitative analysis of the data presented in Fig. 3(a) we extracted the maximum PC (PC_{max}) for different detunings Δ . The normalized values of PC_{max} are plotted in Fig. 3(b) along with theoretical curves calculated according to Eqs. (1) and (2) for different Purcell factors F_P . The experimental data shows a resonance behavior with a pronounced minimum of PC_{max} at $\Delta = 0$. This characteristic can be described quantitatively by our model and allows us to determine F_P . For given values of $\tau_{\text{esc}} = 330 \text{ ps}$, $\tau_{\text{bulk}} = 350 \text{ ps}$,²³ and $\gamma_C = 190 \mu\text{eV}$, we obtain $F_P = 5.2 \pm 0.5$ for the present case. The resonance behavior of the coupled QD-microcavity system was further studied for different excitation powers P . The results are summarized in Fig. 3(c) where the normalized PC_{max} is plotted versus Δ for $P = 30, 180, \text{ and } 600 \mu\text{W}$. Again, the decrease of PC_{max} for $|\Delta| \rightarrow 0$ can clearly be observed, where the resonance character becomes less pronounced with increasing excitation power. This tendency is related to saturation of the QD transition in accordance with Eq. (1). In fact, excellent quantitative agreement between experiment and theory can be achieved and Eq. (2) yields a Purcell factor between 6.5 and 3.1. The decrease of F_P with increasing excitation power is

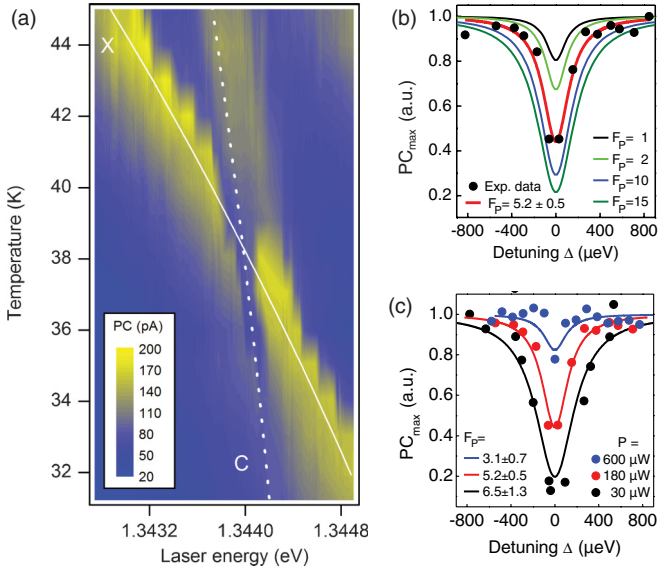


FIG. 3. (Color online) (a) PC intensity map showing the temperature resonance tuning of a QD micropillar with a diameter of $1.8 \mu\text{m}$ and a Q factor of 7000 under side excitation for $P = 180 \mu\text{W}$ and $V_{\text{bias}} = 0 \text{V}$. On resonance between X and C at about 38 K, the PC decreases due to accelerated radiative emission from the QD weakly coupled to the cavity mode. (b) Normalized PC (peak value) as a function of the detuning Δ between X and C. Fitting the experimental data according to Eqs. (1) and (2) (calculated data: solid lines) yields a Purcell factor of 5.2 ± 0.5 . (c) PC resonance behavior for three excitation powers. The experimental data (bullets) is well reproduced by theory (solid lines), which allows the determination of excitation power dependent Purcell factors between 6.5 (for $30 \mu\text{W}$) and 3.1 (for $600 \mu\text{W}$).

attributed to power broadening of the QD transition²⁴ and the related bleaching of the Purcell effect.

Next, we discuss PC features obtained under resonant excitation in the normal direction, where we essentially probe the transmission properties of the coupled QD-microcavity system via electrical readout. Figure 4 compares temperature dependent μPL and μPC spectra recorded from a micropillar with a Q factor of 4200 and a diameter of $1.7 \mu\text{m}$ at $V_{\text{bias}} = 0 \text{V}$ and $P_{\text{ext}} = 210 \mu\text{W}$. In PL [cf. Fig. 4(a)] we observe three QD exciton lines X1–X3 which partially interact with the cavity mode C. In Fig. 4(a) exciton X1 shows the strongest interaction with the cavity mode, which is reflected in an enhancement of emission intensity on resonance due to the Purcell effect. The different interaction strengths of X1–X3 are attributed to different lateral positions of the associated QDs in the active layer,²⁵ where X1 has apparently the highest spatial overlap with the cavity mode. This is in agreement with the μPC spectra depicted in Fig. 4(b) obtained under strict resonant excitation conditions and $P_{\text{ext}} = 30 \mu\text{W}$. Here, only QDs that show significant spatial and spectral overlap with the cavity mode are being excited optically by the transmitted laser light and can contribute to the PC, and thus only X1 is visible in PC. The energy dispersions of the exciton lines and the cavity mode in PL and PC were extracted by Lorentzian line-shape fitting and are plotted in Fig. 4(c). They reveal larger temperature coefficients of the excitonic lines and show a crossing behavior between X1 and X2, respectively, and the cavity mode C.

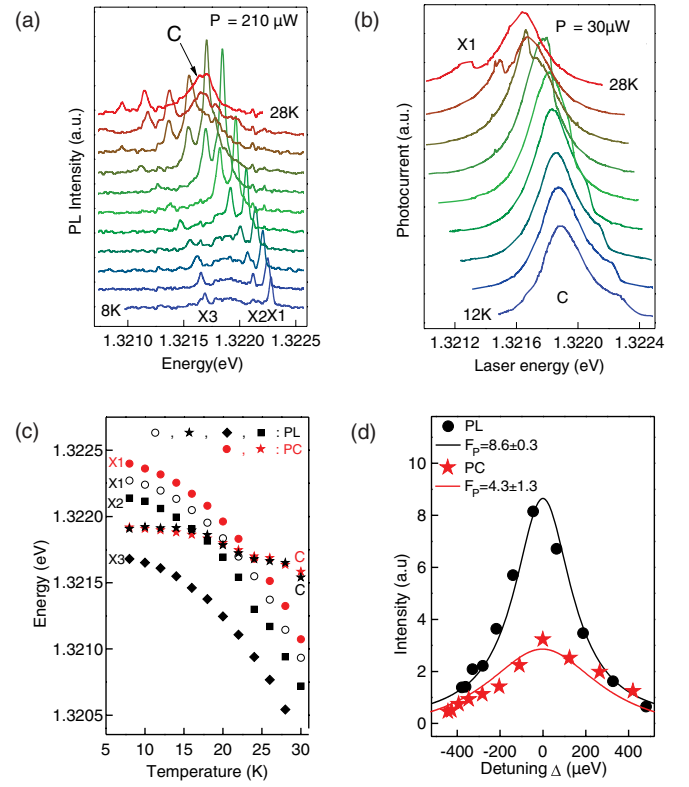


FIG. 4. (Color online) Temperature resonance tuning of a $1.7 \mu\text{m}$ micropillar ($Q = 4200$) under excitation in the normal direction. Temperature dependent set of (a) μPL and (b) μPC spectra at $V_{\text{bias}} = 0 \text{V}$. At resonance with the cavity mode C, the PL and PC intensity of the single QD exciton X1 is strongly enhanced. (c) Energy dispersion of excitons (circles) and cavity mode C (stars) in PL (black symbols) and PC (red symbols). (d) Extracted intensity of X1 in dependence of detuning between X1 and C for PC and PL data, and calculated values (solid lines). Fitting the experimental data yields a Purcell factor of 8.6 (PL) and 4.3 (PC), respectively.

The signal of X1 is slightly redshifted in PL compared to PC, which is attributed to a different electrostatic environment under resonant excitation.

Interestingly, and in contrast to Fig. 3, an enhancement of the PC signal of X1 occurs at resonance with the cavity mode C in Fig. 4(b). In order to describe this finding one needs to take the spectral selectivity of the resonator into account. Indeed, maximum transfer of light into the resonator occurs when the laser wavelength coincides with an optical resonance of the micropillar cavity. In good approximation (in the weak coupling regime) the effective excitation power experienced by a QD exciton detuned by Δ from the cavity mode is given by

$$P(\Delta) = P_{\text{max}} \frac{\gamma_C^2}{4\Delta^2 + \gamma_C^2}, \quad (3)$$

which considers the Lorentzian line shape of the cavity mode. By applying this model, we describe the detuning dependence of the maximum photocurrent under normal excitation of the coupled QD-cavity system in order to determine the associated Purcell factor. As can be seen in Fig. 4(d), very good agreement between experiment (\star) and theory (solid red line) is obtained in PC, and from a fit to the measured data

we extract a Purcell factor $F_P = 4.3 \pm 1.3$. This number is lower than the value ($F_P = 8.6 \pm 0.3$) obtained by modeling the PL data (experiment: ●; theory: black solid line), where the underlying model takes into account that the QD was excited at constant excitation power close to saturation.²⁶ The deviation of F_P could be attributed to significantly different excitation conditions between PL (nonresonant excitation at 842 nm) and PC (resonant excitation) and associated power broadening of the exciton line [cf. Fig. 3(c)]. Nevertheless, the comparison between the two fundamentally different spectroscopic techniques shows again that PC spectroscopy at the single emitter level is a suitable and complementary method to study cQED effects in coupled QD-microcavity systems.

In conclusion, single emitter cQED effects have been investigated in a QD-microcavity system under strict resonant excitation and electrical readout. We identified a competition

between tunnel escape and radiative recombination of a resonantly excited QD interacting with the optical mode of a micropillar cavity. This experimental configuration gives access to light-matter interaction effects at the single emitter level under electrical readout and allows one to precisely determine the Purcell factor for a given excitation power. Our work will pave the way for future studies of coherently coupled systems under electrical readout, emission, and control, which could lead to qubit interconverters in future quantum communication systems.

The authors gratefully thank M. Emmerling and A. Wolf for expert sample preparation and P. Mrowiński for technical assistance. This work was financially supported by the German Ministry of Education and Research (BMBF) via the project QuaHL-Rep and by the State of Bavaria.

*Present address: Institut für Festkörperphysik, Technische Universität Berlin, Hardenbergstraße 36, D-10623 Berlin, Germany.

†stephan.reitzenstein@physik.tu-berlin.de

¹K. J. Vahala, *Nature (London)* **424**, 839 (2003).

²A. J. Shields, *Nat. Photon.* **1**, 215 (2007).

³J. P. Reithmaier, *Semicond. Sci. Technol.* **23**, 123001 (2008).

⁴P. Michler, A. Kiraz, C. Becher, W. V. Schoenfeld, P. M. Petroff, L. Zhang, E. Hu, and A. Imamoglu, *Science* **290**, 2282 (2000).

⁵S. Strauf, N. G. Stoltz, M. T. Rakher, L. A. Coldren, P. M. Petroff, and D. Bouwmeester, *Nat. Photonics* **1**, 704 (2007).

⁶T. Heindel, C. Schneider, M. Lerner, S. H. Kwon, T. Braun, S. Reitzenstein, S. Höfling, M. Kamp, and A. Forchel, *Appl. Phys. Lett.* **96**, 011107 (2010).

⁷D. Press, S. Götzinger, S. Reitzenstein, C. Hofmann, A. Löffler, M. Kamp, A. Forchel, and Y. Yamamoto, *Phys. Rev. Lett.* **98**, 117402 (2007).

⁸K. Hennessy, A. Badolato, M. Winger, D. Gerace, M. Atatüre, S. Gulde, S. Fält, E. L. Hu, and A. Imamoglu, *Nature (London)* **445**, 896 (2007).

⁹D. Englund, A. Faraon, I. Fushman, N. Stoltz, P. Petroff, and J. Vuckovic, *Nature (London)* **450**, 857 (2007).

¹⁰A. B. Young, R. Oulton, C. Y. Hu, A. C. T. Thijssen, C. Schneider, S. Reitzenstein, M. Kamp, S. Höfling, L. Worschech, A. Forchel, and J. G. Rarity, *Phys. Rev. A* **84**, 011803 (2011).

¹¹A. Müller, E. B. Flagg, P. Bianucci, X. Y. Wang, D. G. Deppe, W. Ma, J. Zhang, G. J. Salamo, M. Xiao, and C. K. Shih, *Phys. Rev. Lett.* **99**, 187402 (2007).

¹²S. Ates, S. M. Ulrich, S. Reitzenstein, A. Löffler, A. Forchel, and P. Michler, *Phys. Rev. Lett.* **103**, 167402 (2009).

¹³E. Beham, A. Zrenner, F. Findeis, M. Bichler, and G. Abstreiter, *Appl. Phys. Lett.* **79**, 2808 (2001).

¹⁴R. Oulton, J. J. Finley, A. D. Ashmore, I. S. Gregory, D. J. Mowbray, M. S. Skolnick, M. J. Steer, S.-L. Liew, M. A. Migliorato, and A. J. Cullis, *Phys. Rev. B* **66**, 045313 (2002).

¹⁵A. Zrenner, E. Beham, S. Stuffer, F. Findeis, M. Bichler, and G. Abstreiter, *Nature (London)* **418**, 612 (2002).

¹⁶S. Stuffer, P. Ester, A. Zrenner, and M. Bichler, *Appl. Phys. Lett.* **85**, 4202 (2004).

¹⁷S. Michaelis de Vasconcellos, S. Stuffer, S.-A. Wegner, P. Ester, A. Zrenner, and M. Bichler, *Phys. Rev. B* **74**, 081304 (2006).

¹⁸S. Stuffer, P. Ester, A. Zrenner, and M. Bichler, *Phys. Rev. Lett.* **96**, 037402 (2006).

¹⁹C. Böckler, S. Reitzenstein, C. Kistner, R. Debusmann, A. Löffler, T. Kida, S. Höfling, A. Forchel, L. Grenouillet, J. Claudon, and J. M. Gérard, *Appl. Phys. Lett.* **92**, 091107 (2008).

²⁰M. Kroner, A. O. Govorov, S. Remi, B. Biedermann, S. Seidl, A. Badolato, P. M. Petroff, W. Zhang, R. Barbour, B. D. Gerardot, R. J. Warburton, and K. Karrai, *Nature (London)* **451**, 311 (2008).

²¹S. Ates, S. M. Ulrich, A. Ulhaq, S. Reitzenstein, A. Löffler, S. Höfling, A. Forchel, and P. Michler, *Nat. Photonics* **3**, 724 (2009).

²²A. Andronico, J. Claudon, J.-M. Gérard, V. Berger, and G. Leo, *Opt. Lett.* **33**, 2416 (2008).

²³S. Reitzenstein, S. Münch, P. Franek, A. Rahimi-Iman, A. Löffler, S. Höfling, L. Worschech, and A. Forchel, *Phys. Rev. Lett.* **103**, 127401 (2009).

²⁴A. Ulhaq, S. Ates, S. Weiler, S. M. Ulrich, S. Reitzenstein, A. Löffler, S. Höfling, L. Worschech, A. Forchel, and P. Michler, *Phys. Rev. B* **82**, 045307 (2010).

²⁵S. Reitzenstein, C. Hofmann, A. Löffler, A. Kubanek, J.-P. Reithmaier, M. Kamp, V. D. Kulakovskii, L. V. Keldysh, T. L. Reinecke, and A. Forchel, *Phys. Status Solidi B* **243**, 2224 (2006).

²⁶M. Munsch, A. Mosset, A. Auffèves, S. Seidelin, J. P. Poizat, J.-M. Gérard, A. Lemaître, I. Sagnes, and P. Senellart, *Phys. Rev. B* **80**, 115312 (2009).